

SHALLOW WATER BATHYMETRY WITH AN INCOHERENT X-BAND RADAR USING SMALL (SMALLER) SPACE-TIME IMAGE CUBES

Ron Abileah¹ and Dennis B. Trizna²

¹Omegak, ² Imaging Science Research Inc.

ABSTRACT

The approach most commonly used in bathymetry by “depth inversion” starts by transforming a space-time cube of ocean surface images into a wavenumber-frequency spectrum. The depth is determined by fitting the shallow water gravity wave dispersion equation to the 3D spectrum. The depth error using this method is inversely proportional to the image cube size. Very large image cubes are required for accurate bathymetry. Typical cube dimensions are on the order of 250 m x 250 m x 100 s. A new algorithm, originally developed for satellite images, can achieve the same accuracy with much smaller cubes, on the order of 100 m x 100 m x 10 s. This paper describes a test of this algorithm on low grazing angle radar data. The algorithm offers the potential for rapid near shore bathymetry surveys using marine X-band radars flown on aircraft.

Index Terms— Marine radar, sea coast, algorithms

1. INTRODUCTION

Since this paper is in the IGARSS special session by the title “Ocean Radar Remote Sensing at Grazing Incidence” it is apropos that we recall one of the key experiments in the early days of this field of research. The experiment was also first reported at (coincidentally!) an IGARSS conference. In late 1984 investigators from the Netherlands Organization for Applied Scientific Research (TNO) installed an experimental X-band marine radar on the dunes of Scheveningen beach to record an image cube of radar backscatter from shoaling waves. Their analysis of the data turned out to be the first demonstration of depth inversion with radar imagery [1] and Prof. Hoozeboom’s presentation of this experiment at IGARSS’86 [2] was honored with the best paper award in that conference. His paper also inspired the research that eventually led to the study reported here.

In all the subsequent improvements on the original Dutch work (Bell [3], Trizna [4], Senet et al. [5], and the AROSS project [6], to mention just a few), there has been one constant in the processing methodology: all start with a space-time image cube Fourier transformed into a wavenumber-frequency power spectrum. The various

implementations differ mostly in the details of processing after the 3D Fourier transform.

The accuracy achieved with these algorithms is very dependent on the wavenumber and frequency resolution of the Fourier transform, which in turn depends on the space-time dimensions of the image cube. The space dimensions are typically $L \times L = 250 \text{ m} \times 250 \text{ m}$; the time dimension, also referred to as the dwell time, is typically $T = 100 \text{ s}$.

An alternative to the 3D approach was conceived and developed by the first author to apply the depth inversion method with IKONOS satellite images [7]. The IKONOS satellite has a fast (relative to other commercial satellites) camera re-pointing enabling the capture of two images of the same area within a 13 s interval. Two such images are not sufficient for depth inversion with the traditional 3D Fourier transform approach because the dwell time is too short and the sampling time causes frequency aliasing of the wave spectrum. The new algorithm, however, overcomes these limitations. In the test case with two IKONOS images the depth rms errors were 7% of actual depth, which is comparable to or even better than previous published results with large 3D cubes.

In late 2009 the two authors collaborated on testing the new algorithm with low grazing angle radar data. The purpose was to test the potential for bathymetry with small X-band radars on aircraft or UAVs. The typical dwell time for aircraft would be $\sim 10 \text{ s}$, much less than the 100 s cubes used in 3D algorithms. The goal of the test, therefore, was to determine the performance of the new algorithm on radar data with T as low as 10 s.

The data for this test was collected with the Imaging Science Research radar located on the pier of the U.S. Army Corps of Engineers Field Research Facility, Duck, NC, as further described by Trizna in Reference [8].

2. THE 3D DEPTH INVERSION ALGORITHM

We will refer to the standard algorithms as “3D” because they start with a 3D Fourier transform. The new algorithm is distinguished as “2D” because it uses 2D Fourier transforms.

The following brief review of the 3D is a useful prelude to explaining the 2D. The 3D, as first introduced by

the TNO team and refined in subsequent efforts, starts with a space-time cube of N ocean images $\{S_1(\vec{x}), S_2(\vec{x}), \dots, S_N(\vec{x})\}$. The images dimensions are $L \times L$ taken at intervals τ so that the dwell time is $T = N\tau$. The cube is transformed into a wavenumber (\vec{k})-frequency (ω) power spectrum with a 3D Fourier transform, \mathfrak{S}_3 ,

$$P(\vec{k}, \omega) = |\mathfrak{S}_3[\{S\}]|^2.$$

The energy of linear gravity waves is concentrated in a shell described by

$$\omega_0(\vec{k} | d, \vec{u}) = \sqrt{g |k| \tanh(|k|d)} - \vec{k} \cdot \vec{u}.$$

The depth, d , and the ocean current vector, \vec{u} , are estimated by finding the “best fit” of this equation to the measured power spectrum, P .

The best fit solution is usually found by seeking to minimize some objective function, J_{3D} , on the power spectrum. For example, Tang et al. [9] use

$$\text{argmin}_{d, \vec{u}} J_{3D} = \dots \\ \sum_{k_x, k_y} W(\vec{k}) \sum_{\omega} (\omega - \omega_0(\vec{k} | d, \vec{u}))^2 P(\vec{k}, \omega).$$

$W(\vec{k})$ is an optional wavenumber weighting filter that can be used to give greater weight or filter out certain regions of the wavenumber space. For example, it can be used to notch out wind modulations, nonlinear harmonics (see discussion in Section 5), and other noise sources.

The 3D algorithm is at best an approximation and must be used with some care and appreciation of its limitations. There is an implicit assumption in 3D that depth is constant over the area $L \times L$. Also implicit in the approach is that waves do not refract appreciably in the time interval T , which is only strictly true for waves traveling exactly perpendicular to the bottom slope. One way out of these assumptions is to use smaller cube dimensions, but this leads to poorer spectral resolution and less accuracy in the bathymetry. Piotrowski and Dugan [6, section IV] show that the depth accuracy is $\propto T^{-1}$ and $\propto L^{-1}$, based both on theory and real data.

3. THE 2D ALGORITHM

The 2D algorithm begins with the 2-D Fourier transforms, \mathfrak{S}_2 , of each of the N images,

$$F_n(\vec{k}) = \mathfrak{S}_2[S_n]$$

A propagation kernel is defined as,

$$\Phi_{\pm}(k_x, k_y | d, \vec{u}) \equiv e^{\pm i \alpha_0(k_x, k_y | d, \vec{u}) \tau}.$$

The sign in the exponent depends on whether the waves are travelling in +x or -x. For gravity waves the Fourier transform at time step n is simply related to another at time step $n+m$ by the equation $F_{n+m} = \Phi^m F_n$. The wave direction can be determined from the sign that provides the greatest coherence between pairs of images, i.e.,

$$\langle (\Phi_+ F_n)^* F_{n+1} \rangle \text{ vs. } \langle (\Phi_- F_n)^* F_{n+1} \rangle.$$

A variety of useful objective functions can be formulated from the $F_{n+m} = \Phi^m F_n$ relationship for any number of images $N \geq 2$. For example the following seeks to minimize the differences between image pairs,

$$\text{argmin}_{d, \vec{u}} J_{\Delta} = \sum_{k_x, k_y} W(\vec{k}) \sum_{n=1}^{N-m} |F_{n+m} - \Phi^m F_n|^2.$$

Usually differences are taken between consecutive images ($m = 1$). However the method permits other values for m which may be advantageous in some cases.

Another possible objective function seeks the maximum coherent sum of the N images,

$$\text{argmax}_{d, \vec{u}} J_{\Pi} = \sum_{k_x, k_y} W(\vec{k}) \left| \sum_{n=1}^N \Phi^{-n} F_n \right|^2.$$

This is closely related to the 3D algorithms but without the requirement for large number of images or long dwell time.

Figure 1 compares J_{Δ} to J_{Π}^{-1} on simulated ocean waves propagating over a constant depth of 7 m. (Note, the inverse is used to facilitate comparison of the minima in the first with the maximum in the latter.) Both show a deep minimum at the correct depth. This plot is for $N = 2$ and $\tau = 1$ s but these functions are independent of N and τ when there is no noise.

On real radar data (described in following sections) these objective functions behaved similarly, but the minima locations are affected by noise. When the signal-to-noise ratio (SNR) is very high the two minima are generally very close.

The J_{Δ} form was used for all subsequent analysis.

There are several benefits to J_{Δ} relative to J_{3D} . As already mentioned, depth can be estimated with as few as two frames, which was the particular attraction for IKONOS satellite imagery. But more importantly, the depth accuracy does not depend on T , the frequency resolution is not relevant. Accuracy depends only on the SNR. The SNR can be managed to a great extent by sensor design (e.g., choice of radar power, range, antenna gain, HH vs VV polarization) sensor geometry (grazing angle, alignment of radar view with respect to the wind), and wavenumber filters (see section 5). If the SNR is sufficiently high the depth can be determined very precisely with a few images

and short dwell time. Another benefit is that J_{Δ} is only sensitive to wave motion over the time interval $m\tau$ (which is usually order of a second or a few seconds), as compared to 3D where the wave motion is over the dwell time (order of 100 seconds). Therefore the method is less susceptible to the “smear effect” from waves propagating (and refracting) over a sloping bottom .

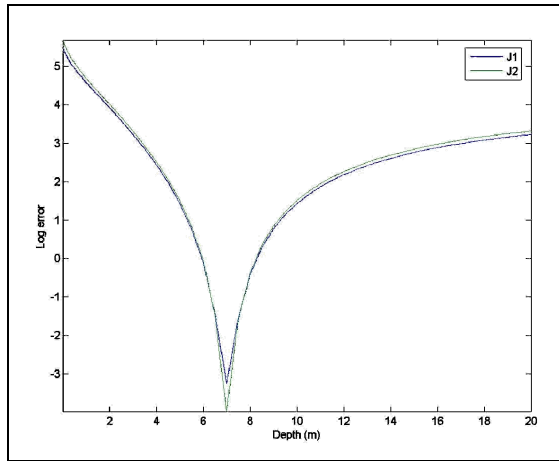


Figure 1 Objective functions with simulated waves propagating over a constant 7 m depth, plotted for depth (x-axis) varying from 0 to 20 m. Blue curve is $\log J_{\Delta}$, green (lower) curve is $-\log J_{\Pi}$. The minima are at 7 m.

4. DESCRIPTION OF THE RADAR DATA

The data used for the test was collected on November 29, 2009 with a standard incoherent 12-kW Kodan radar with 6' antenna. The radar was modified to access the video signal, heading pulse and azimuthal position counter, and all were simultaneously recorded for accurate Cartesian registration. Transmit pulse length was 80 ns, or 12 m long, with some pulse shaping to permit higher resolution.

All video pulse echoes received each 0.5 ms were recorded and digitized at a 50 MHz rate. Pulse echoes were summed on the acquisition board and recorded at 12 bits at azimuthal intervals of one half the radar beam width. The rotation period of the radar is 1.25-s. Each rotation produces one 360° radar image. For this test the range-azimuth data were interpolated to Cartesian co-ordinates at 3-m resolution. The data set was 66 images (66 rotations, 83 s). Reference [8] has examples of the standard products produced with this radar.

Wind and wave conditions were mild during this data collection. The significant wave height was 0.33 m, wave direction 62° (approximately on-shore), wave period 7 s; wind speed was 3.8 m/s, heading 260°.

5. BATHYMETRY FROM THE RADAR DATA

The 66 radar images available for this study were grouped for processing with $N = 8, 16, 32,$ and 66. The corresponding dwell times are 10, 20, 40, and 83 s, respectively. The spatial dimension (L) was held constant at 100 m.

One important caveat to all the foregoing results: the radar range resolution is insufficient to resolve the short waves needed by the algorithm to estimate the current. So we assume the current is alongshore and zero in the wave direction (which was primarily onshore). This assumption would introduce a bias in the estimated depth if there was in fact a significant onshore current.

Figure 2 is a typical bathymetry map output with $N = 16$. The bathymetry, color coded from 1 m (blue) to 14 m (dark red), is shown superimposed on an aerial image of the FRF and Duck, NC. Some of the outputs are eliminated from further analysis. One area is a circular zone of 100 m

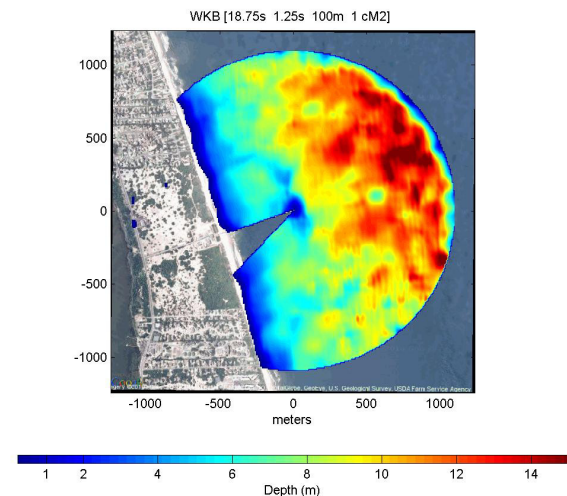


Figure 2 Bathymetry derived with $N=16$.

centered on the radar, and another of a similar size centered on an instrument buoy to the right. Edge effects on the circumference of the radar footprint are also disregarded.

Figure 3 is the joint probability of solutions as a function of cross-shore distance and depth. At FRF the depth contours are approximately parallel with the shore so the depth variability at any fixed cross-shore distance can be interpreted as an *upper bound* on the variability in the depth solution at a particular fixed depth. The apparent variability in depth estimates increases with depth. At 500 m from shore, where the depth is approximately 7 m, the standard deviation is 1.3 m (for $N=8$), 1.0 m (16), 0.82 m (32), and 0.65 m (66). The standard deviation has only *doubled* in decreasing N from 66 to 8. Reference [6] predicts that the error would have increased *8-fold* with the 3D algorithm. This test result implies that the error with the 2D is not

dependent on frequency resolution. Furthermore it shows that 2D can be used with radar data and T as small as 10 s.

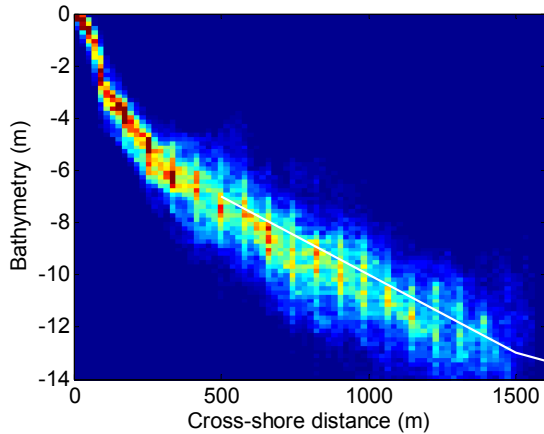


Figure 3 Bathymetry for $N=16$. The white line is the historical FRF depth profile.

6. DISCUSSION OF NONLINEARITIES

A number of previous researchers, e.g., Nieto Borge et al. [10], have pointed out various non-linearities that can affect radar imaging of ocean waves. The energy from non-linearities can fall outside the gravity wave dispersion shell and leads to biases in the depth solution. The nonlinearities are more pronounced in low grazing angles.

The 3D algorithms have the potential to filter out the nonlinear energy by frequency filtering [10], the better with longer T . This gives the 3D method a possible advantage over 2D. However, it appears not to be a significant advantage. In most cases the nonlinear energy is separable from linear gravity wave energy in both frequency and wavenumber. The 2D can not filter in frequency but can filter in wavenumber with the $W(\vec{k})$ weighting. The following was used for results in this paper. First the coherence-magnitude-square $\Lambda(\vec{k})$ was estimated from one or more image pairs. The signal-to-noise ratio is $\Gamma = \Lambda / (1 - \Lambda)$. Using $W = \Gamma$ greatly improved the wave contrast, typically by more than 10 dB, and improved the depth accuracy. Furthermore the peak ocean wave wavenumber, k_0 , was determined from the peak in Γ and $W(\vec{k})$ was truncated at wavenumbers $> 2k_0$ and $< k_0 / 2$. The truncation eliminates harmonics, sub-harmonics, and other superfluous noise.

Ultimately a better way to avoid most non-linear effects is to operate the sensor at somewhat higher grazing angles. This is easier from an aircraft than ship or tower.

7. CONCLUSION

Our test showed that the 2D algorithm can be used with a nautical X-band radar to map bathymetry with as short a dwell time as 10 s. This can be useful for rapid bathymetry surveys from an aircraft. With the 3D methods the aircraft would need to fly very slowly or in circles (e.g., see [6]) to dwell for 100 s on a fixed patch of the ocean. With the 2D method the dwell time can be reduced to 10 s so the aircraft can fly faster and parallel to the coast. The entire CONUS coast could be surveyed with a small aircraft in 40 hours of flight time.

8. REFERENCES

- [1] D. van Halsema, D., and J. C. M. Kleyweg, "The measurement of wavefields with a simple ship's radar," Fysisch En Electronisch Laboratorium, TNO, Report FEL, 20 April 1986 (in Dutch)
- [2] P. Hoogeboom, J. C. M. Kleijweg, and D. van Halsema, "Seawave measurements using ship's radar," Proc. IGARSS Symp., 8–11 September 1986
- [3] P. S. Bell, "Bathymetry derived from an analysis of X-band marine radar images of waves," Proc. Oceanology '98, vol. 3, pp. 535–543, 1998
- [4] D. Trizna, "Errors in Bathymetric Retrievals Using Linear Dispersion in 3-D FFT Analysis of Marine Radar Ocean Wave Imagery," IEEE Transactions on Geoscience and Remote Sensing, vol. 39, No. 11, November 2001
- [5] C. M. Senet, J. Seemann, S. Flampouris, and F. Ziemer, "Determination of Bathymetric and Current Maps by the Method DiSC Based on the Analysis of Nautical X-Band Radar Image Sequences of the Sea Surface," IEEE Transactions on Geoscience and Remote Sensing, Volume 46, No. 8, Aug. 2008
- [6] C. C. Piotrowski, and J. P. Dugan, "Accuracy of Bathymetry and Current Retrievals From Airborne Optical Time-Series Imaging of Shoaling Waves," IEEE Transactions on Geoscience and Remote Sensing, Vol. 40, No. 12, December 2002
- [7] R. Abileah, "Mapping Shallow Water Depth from Satellite," ASPRS 2006 Annual Conference, Reno, Nevada May 1-5, 2006
- [8] D. M. Trizna, www.frf.usace.army.mil/radar/
- [9] Y. Tang, Y. Hao, and Z. Lu, "Ocean Surface Currents Determination from X-Band Radar Image Sequences," Proceedings of the 2008 International Workshop on Education Technology and Training & 2008 International Workshop on Geoscience and Remote Sensing, 1, 320-323, 2008
- [10] J. C. Nieto Borge and C. Guedes Soares, "Analysis of directional wavefields using X-band navigation radar," Coastal Engineering 40, 375–391, 2000